Supplementary information

Supplemental Figure S1: Loss of *Tfb2m* in β-cells results in changes in apoptotic markers, reduced β-cell mass, and reduced islet density. (a) Western blot and densitometry analysis of cleaved-caspase 3, cleaved-caspase 9, and BAX:BCL-2 protein abundance in in islets from control and β-*Tfb2m*$^{-/-}$ mice; control, *n*=6 mice and β-*Tfb2m*$^{-/-}$, *n*=5 mice. (b and c) Quantification of β-cell mass and islet density in control and β-*Tfb2m*$^{-/-}$ mice at 7 weeks of age, *n*=6 mice. Representative images for quantitative western blots are shown. All data are mean ± s.e.m. Statistical differences were examined by unpaired Student's t-test. *P<0.05 and **P<0.01 versus the corresponding value for control mice.

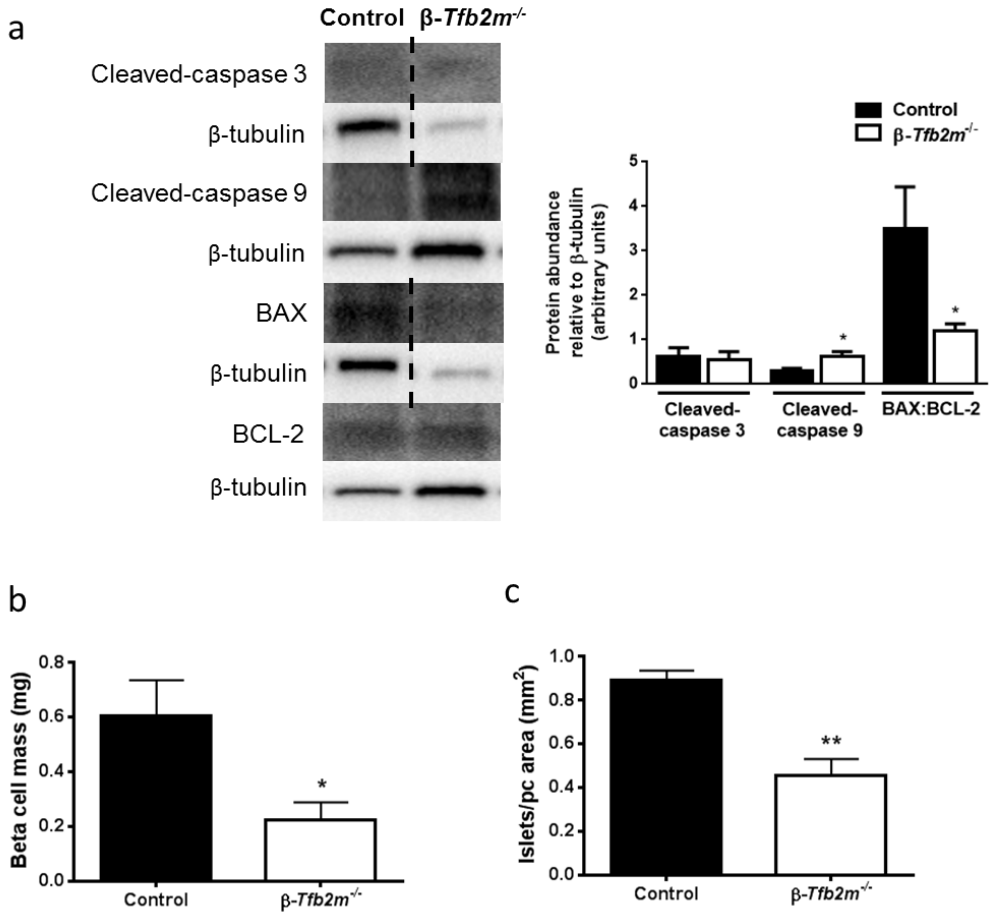

Supplemental Figure S2: Heterozygous loss of *Tfb2m* in β-cells results in disrupted whole body metabolism as a consequence of impaired mitochondrial function and diminished insulin secretion. qRT-PCR analysis of (a) *Tfb2m* and *Tfam* mRNA and (b) mitochondrial genes in islets from control and β-*Tfb2m*$^{+/-}$ mice; control, *n*=4 mice and β-*Tfb2m*$^{+/-}$, *n*=6 mice. Plasma (c) glucose and (d) insulin concentrations in non-fasted control and β-*Tfb2m*$^{+/-}$ mice at seven months of age; control, *n*=4 mice and β-*Tfb2m*$^{+/-}$, *n*=5 mice. (e) Calculation of the area under the curve (AUC) for plasma glucose during an IVGTT in control and β-*Tfb2m*$^{+/-}$ mice at six months of age; control, *n*=4 mice and β-*Tfb2m*$^{+/-}$, *n*=5 mice. (f) Calculation of insulin response defined as AUC for plasma insulin from 0 to 5 mins during an IVGTT in control and β-*Tfb2m*$^{+/-}$ mice at six months of age; control, *n*=4 mice and β-*Tfb2m*$^{+/-}$, *n*=5 mice. (g) Change in TMRM fluorescence intensity from baseline following stimulation with 16.7 mM glucose of islets from control and β-*Tfb2m*$^{-/-}$ mice at seven months of age, *n*=4 mice. (h and i) Islet ATP content at 1.8 mM glucose and upon stimulation with 22 mM glucose in control and β-*Tfb2m*$^{+/-}$ mice at seven months of age; control, *n*=6 mice and β-*Tfb2m*$^{+/-}$, *n*=10 mice (j) Insulin secretion from islets in control and β-*Tfb2m*$^{+/-}$ mice at seven months of age. Islets were incubated for 1 h in 2.8 mM and 16.7 mM glucose, 10 mM α-ketoisocaproic acid (α-KIC), and 2.8 mM glucose with 35 mM potassium chloride (KCl); control, *n*=4 mice, β-*Tfb2m*$^{+/-}$, *n*=5 mice. (k) Pancreatic insulin content per weight of pancreas in control and β-*Tfb2m*$^{+/-}$ mice at seven months of age; control, *n*=3 mice, β-*Tfb2m*$^{+/-}$, *n*=5 mice. All data are mean ± s.e.m. Statistical differences were examined by unpaired Student's t-test. *P<0.05, **P<0.01 and ***P<0.001 versus the corresponding value for control mice.

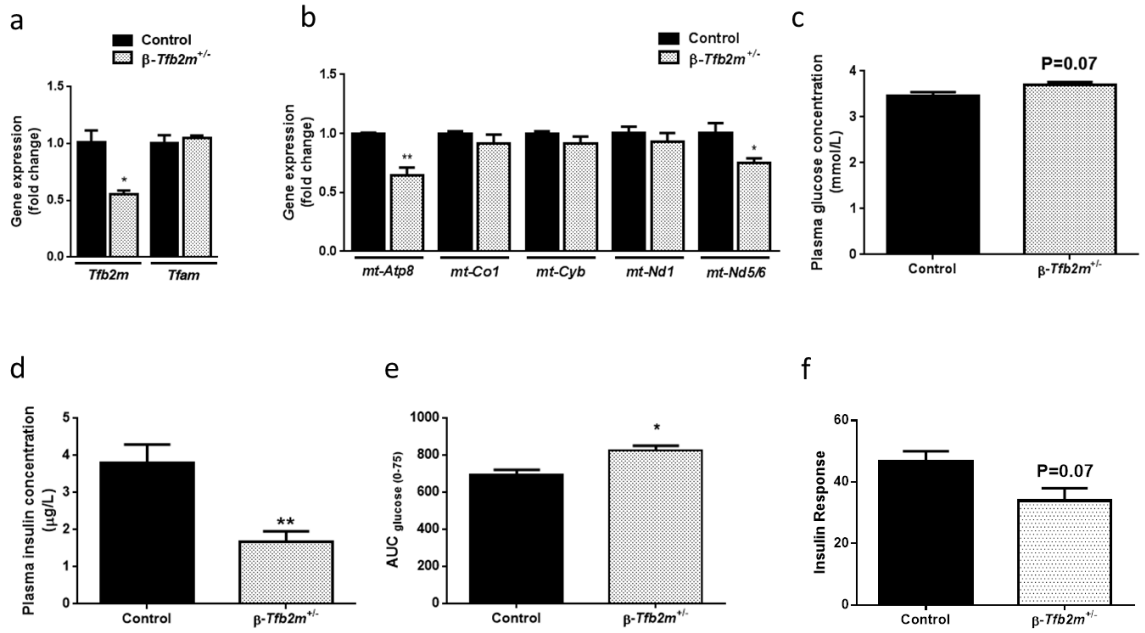

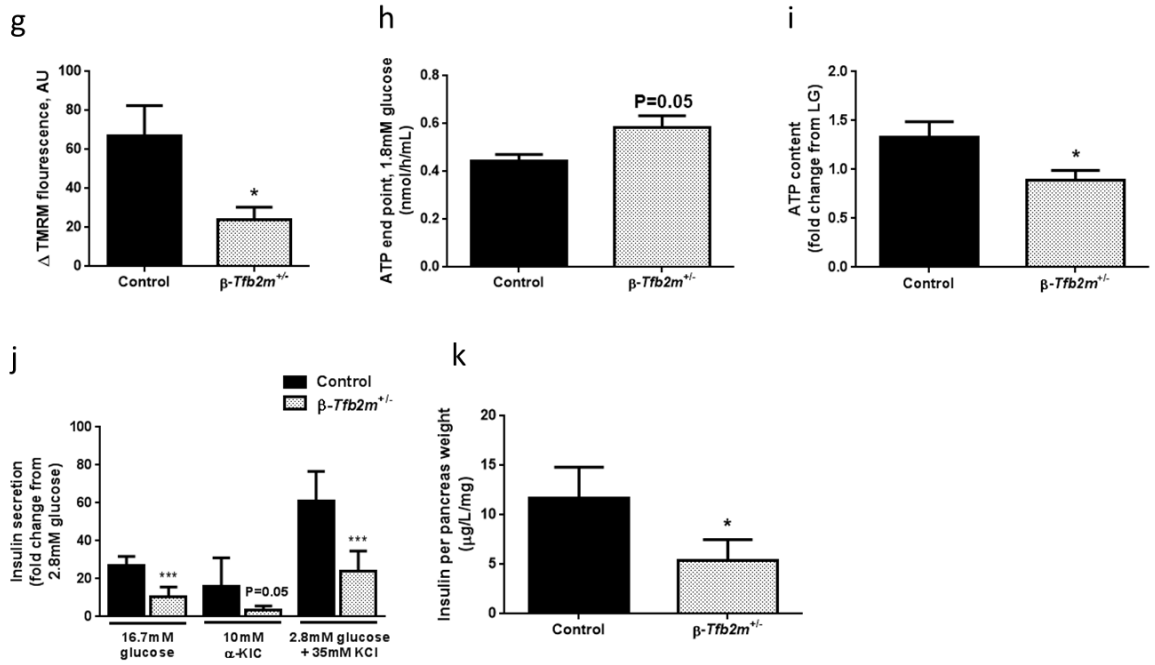
g
Δ TMRM flourescence, AU
100
80
60
40
20
0
*
Control
β-Tfb2m+/-
h
ATP end point, 1.8mM glucose (nmol/h/mL)
0.8
0.6
0.4
0.2
0.0
P=0.05
Control
β-Tfb2m+/-
i
ATP content (fold change from LG)
2.0
1.5
1.0
0.5
0.0
*
Control
β-Tfb2m+/-
j
Control
β-Tfb2m+/-
Insulin secretion (fold change from 2.8mM glucose)
100
80
60
40
20
0
***
P=0.05
***
16.7mM glucose
10mM α-KIC
2.8mM glucose + 35mM KCl
k
Insulin per pancreas weight (µg/L/mg)
20
15
10
5
0
*
Control
β-Tfb2m+/-

Supplemental Figure S3: Silencing of *TFB2M* in insulin-producing cells results in decreased expression of mitochondrial encoded genes and consequently impaired insulin secretion. (a) qRT-PCR analysis of *TFB2M* mRNA (left; *n*=9 different cell passages/group) and western blot and densitometry analysis of TFB2M protein abundance (right; *n*=3 different cell passages/group) in control and *TFB2M*-deficient INS-1 832/13 clonal cells. (b) qRT-PCR analysis of *TFAM* mRNA (left; *n*=9 different cell passages/group) and western blot and densitometry analysis of TFAM protein abundance (right; *n*=5 different cell passages/group) in control and *TFB2M*-deficient INS-1 832/13 clonal cells. (c) qRT-PCR analysis of mitochondrial encoded genes in control and *TFB2M*-deficient INS-1 832/13 clonal cells; *n*=9 different cell passages /group. (d) Western blot and densitometry analysis of NDUFB8, MT-ND1, SDHB, UQCRC2, MT-CO1, and ATP5A protein abundance in control and *TFB2M*-deficient INS-1 832/13 clonal cells; *n*=5 different cell passages/group. (e and f) Mitochondrial DNA content and citrate synthase activity in control and *TFB2M*-deficient INS-1 832/13 clonal cells; *n*=9 different cell passages/group. (g) Insulin secretion from control and *TFB2M*-deficient INS-1 832/13 clonal cells that were incubated for 1 h in 2.8 mM and 16.7 mM glucose, 10 mM pyruvate, 10 mM leucine/glutamine and 2.8 mM glucose with 35 mM potassium chloride (KCl); *n*=12 different cell passages/group. Representative images for quantitative western blots are shown. All data are mean ± s.e.m. Statistical differences were examined by unpaired Student's t-test *P<0.05, **P<0.01, ***P<0.001 and ****P<0.0001 versus the corresponding value for controls.

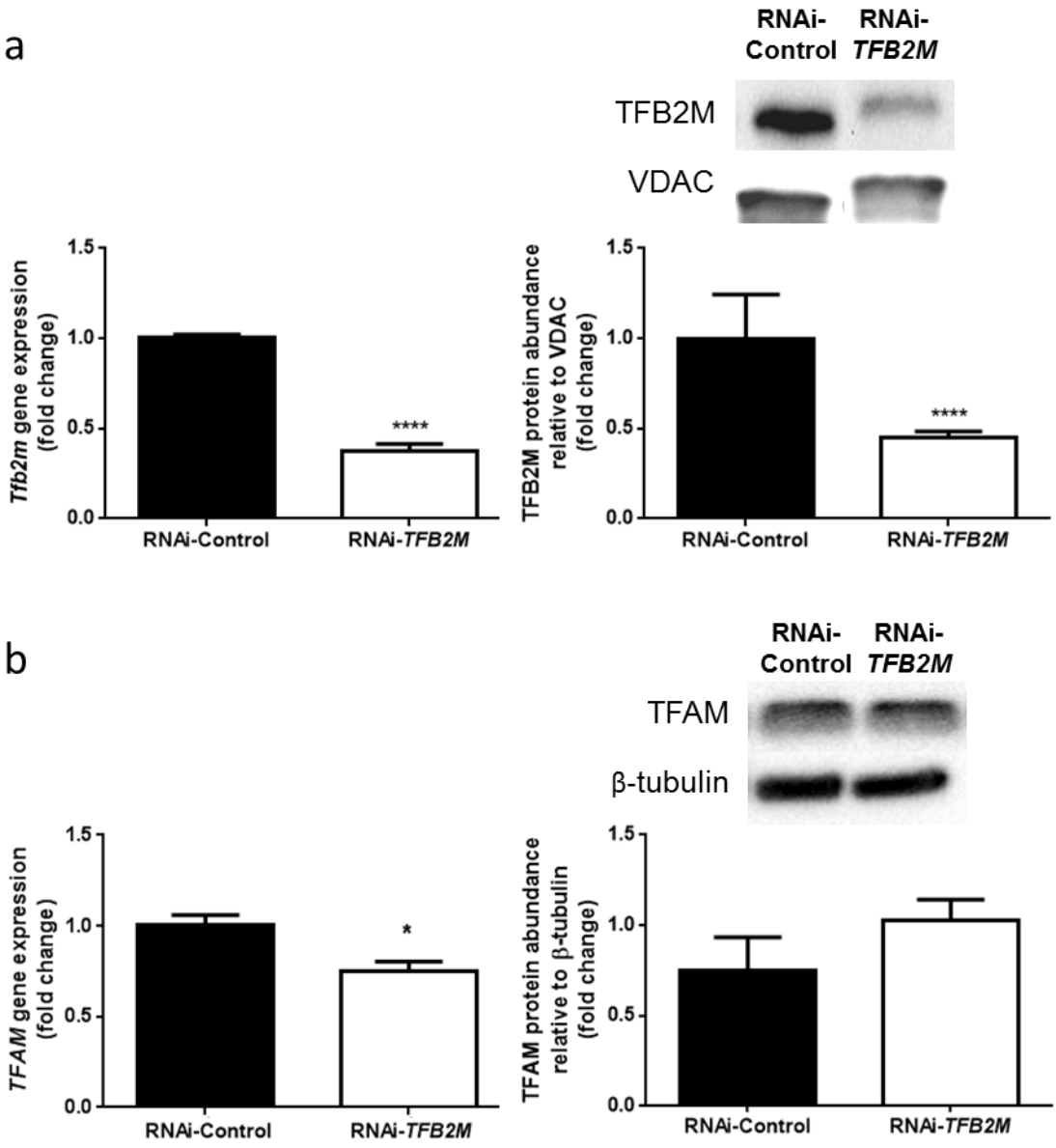
a
RNAi-Control
RNAi-TFB2M
TFB2M
VDAC
Tfb2m gene expression (fold change)
1.5
1.0
0.5
0.0
****
RNAi-Control
RNAi-TFB2M
TFB2M protein abundance relative to VDAC (fold change)
1.5
1.0
0.5
0.0
****
RNAi-Control
RNAi-TFB2M
b
RNAi-Control
RNAi-TFB2M
TFAM
β-tubulin
TFAM gene expression (fold change)
1.5
1.0
0.5
0.0
*
RNAi-Control
RNAi-TFB2M
TFAM protein abundance relative to β-tubulin (fold change)
1.5
1.0
0.5
0.0
RNAi-Control
RNAi-TFB2M

c

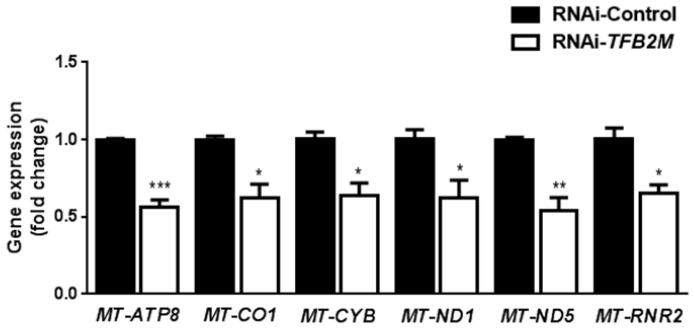
RNAi-Control
RNAi-TFB2M
Gene expression (fold change)
1.5
1.0
0.5
0.0
***
*
*
*
**
*
MT-ATP8
MT-CO1
MT-CYB
MT-ND1
MT-ND5
MT-RNR2

d

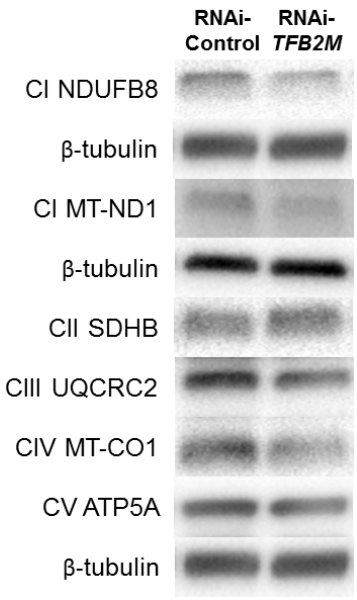
RNAi-Control
RNAi-TFB2M
CI NDUFB8
β-tubulin
CI MT-ND1
β-tubulin
CII SDHB
CIII UQCRC2
CIV MT-CO1
CV ATP5A
β-tubulin

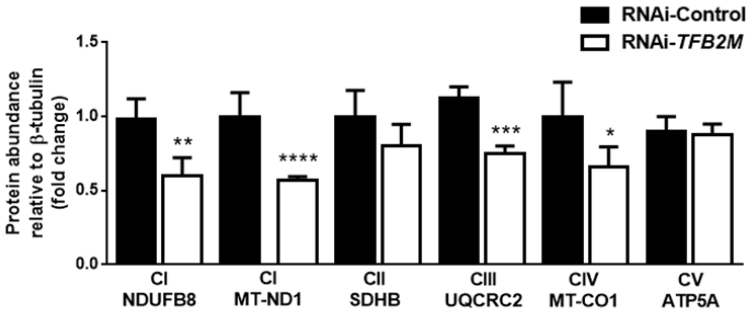
RNAi-Control
RNAi-TFB2M
Protein abundance relative to β-tubulin (fold change)
1.5
1.0
0.5
0.0
**
****
***
*
CI NDUFB8
CI MT-ND1
CII SDHB
CIII UQCRC2
CIV MT-CO1
CV ATP5A

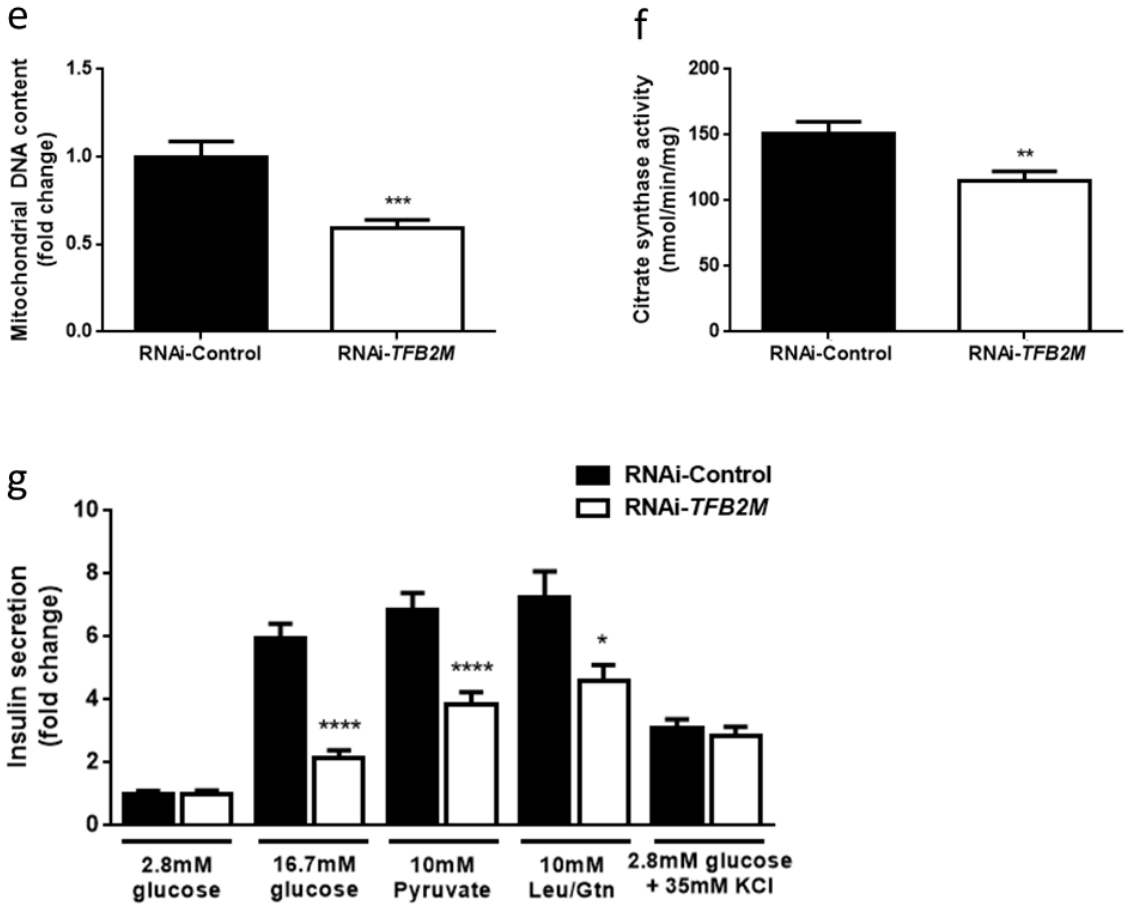
e
Mitochondrial DNA content (fold change)
1.5
1.0
0.5
0.0
***
RNAi-Control
RNAi-TFB2M
f
Citrate synthase activity (nmol/min/mg)
200
150
100
50
0
**
RNAi-Control
RNAi-TFB2M
g
RNAi-Control
RNAi-TFB2M
Insulin secretion (fold change)
10
8
6
4
2
0
****
****
*
2.8mM glucose
16.7mM glucose
10mM Pyruvate
10mM Leu/Gtn
2.8mM glucose + 35mM KCl

Supplemental Figure S4: Silencing of *TFB2M* in insulin-producing cells results in impaired autophagy. (a) Left - Representative fluorescence microscopy image of control and *TFB2M*-deficient INS-1 832/13 clonal cells expressing LC3-GFP (green). Scale bars, 10 μm. Right - Quantification of $LC3^+$ puncta in control and *TFB2M*-deficient INS-1 832/13 clonal cells; *n*=4 different cell passages/group. (b) qRT-PCR analysis of *BECN1*, *CTSB*, and *LAMP2* mRNA in control and *TFB2M*-deficient INS-1 832/13 clonal cells; *n*=5 different cell passages/group. (c) Left - Representative fluorescence microscopy image of control and *TFB2M*-deficient INS-1 832/13 clonal cells expressing LC3-GFP (green) after treatment with Lysotracker (red). Nucleus stained with DAPI (blue). Scale bars, 10 μm. Right - Quantification of $LC3^+$ puncta co-localized with Lysotracker in control and *TFB2M*-deficient INS-1 832/13 clonal cells; *n*=4 different cell passages/group. (d) qRT-PCR analysis of *DDIT3* and *CEBPB* mRNA in control and *TFB2M*-deficient INS-1 832/13 clonal cells; *n*=5 different cell passages/group. All data are mean ± s.e.m. Statistical differences were examined by unpaired Student's t-test. *P<0.05, **P<0.01, ***P<0.001 and ****P<0.0001 versus the corresponding value for controls

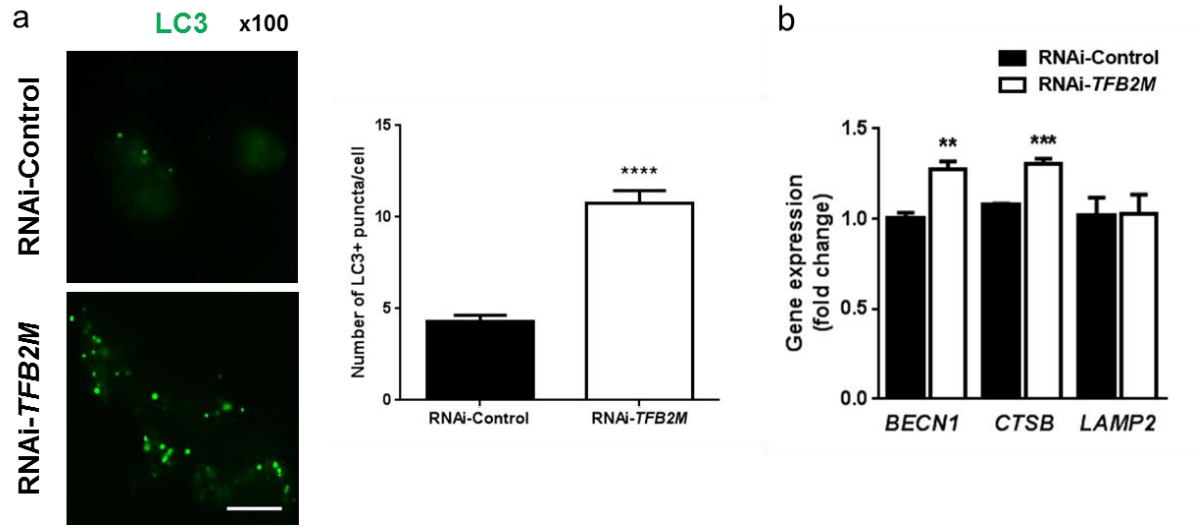

c

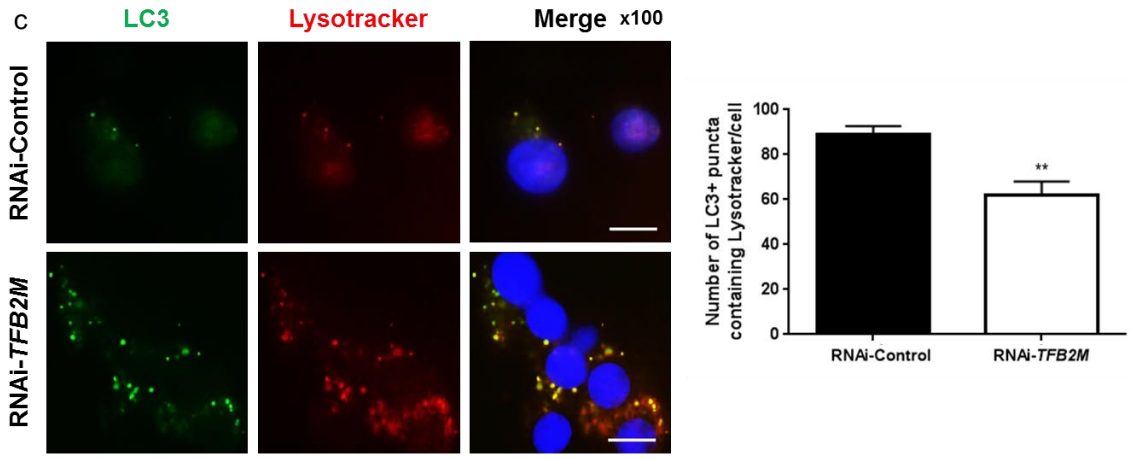
LC3
Lysotracker
Merge x100
RNAi-Control
RNAi-TFB2M
Number of LC3+ puncta containing Lysotracker/cell
100
80
60
40
20
0
**
RNAi-Control
RNAi-TFB2M

d

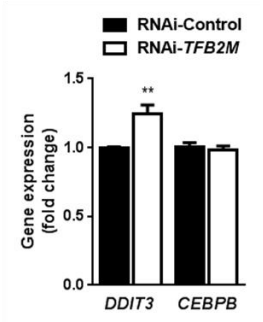
RNAi-Control
RNAi-TFB2M
Gene expression (fold change)
1.5
1.0
0.5
0.0
**
DDIT3
CEBPB

Supplemental Figure S5: Silencing of *TFB2M* in insulin-producing cells results in disruption of the mitochondrial unfolded protein response and impaired mitophagy (a) qRT-PCR analysis of *CLPP* and *HSP60* mRNA and western blot and densitometry analysis of CLPP and HSP60 protein abundance in control and *TFB2M*-deficient INS-1 832/13 clonal cells; *n*=5 different cell passages/group. (b) Left - Representative fluorescence microscopy image of control and *TFB2M*-deficient INS-1 832/13 clonal cells expressing LC3-GFP (green) after treatment with Mitotracker (red). Nucleus stained with DAPI (blue). Scale bars, 10 μm. Right - Quantification of $LC3^{+}$ puncta co-localized with Mitotracker in control and *TFB2M*-deficient INS-1 832/13 clonal cells; *n*=4 different cell passages/group. (c) Western blot and densitometry analysis of PINK1 and PARKIN protein abundance in control and *TFB2M*-deficient INS-1 832/13 clonal cells; *n*=5 different cell passages/group. (d) qRT-PCR analysis of *PDX1*, *INS1*, *INS2*, and *SLC2A2* mRNA in control and *TFB2M*-deficient INS-1 832/13 clonal cells; *n*=5 different cell passages/group. Representative images for quantitative western blots are shown. All data are mean ± s.e.m. Statistical differences were examined by unpaired Student's t-test. *P<0.05, **P<0.01, ***P<0.001 and ****P<0.0001 versus the corresponding value for controls

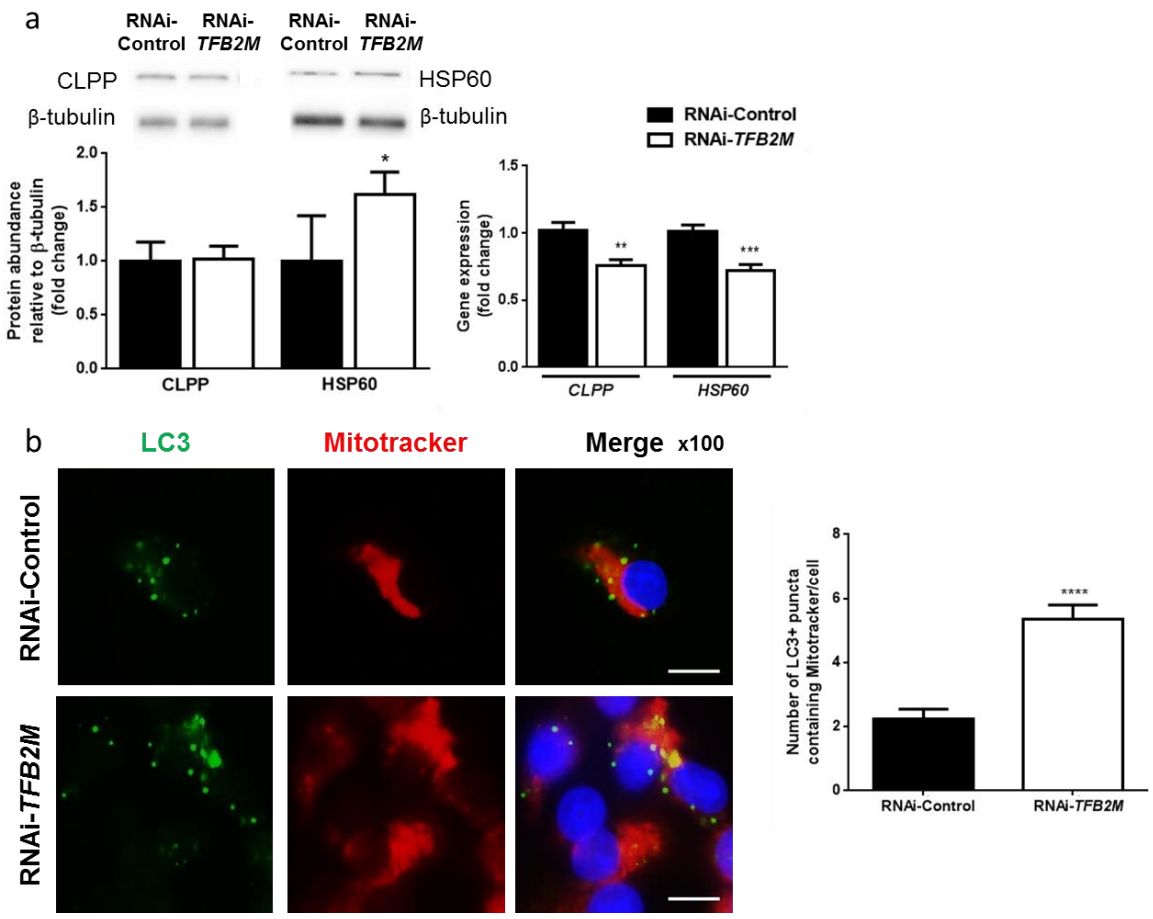

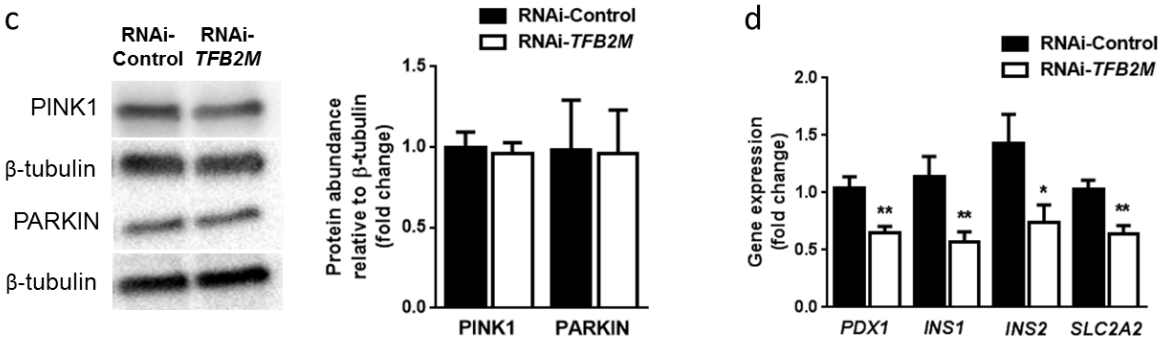
c
RNAi-Control
RNAi-TFB2M
PINK1
β-tubulin
PARKIN
β-tubulin
RNAi-Control
RNAi-TFB2M
Protein abundance relative to β-tubulin (fold change)
1.5
1.0
0.5
0.0
PINK1
PARKIN
d
RNAi-Control
RNAi-TFB2M
Gene expression (fold change)
2.0
1.5
1.0
0.5
0.0
**
**
*
**
PDX1
INS1
INS2
SLC2A2